ORIGINAL ARTICLE

Intrapatient Comparison of ^{111}In-PSMA I&T SPECT/CT and Hybrid ^{68}Ga-HBED-CC PSMA PET in Patients With Early Recurrent Prostate Cancer

Isabel Rauscher, MD,* Tobias Maurer, MD,† Michael Souvatzoglou, MD,*‡ Ambros J. Beer, MD,‡
Tibor Vag, MD,* Martina Wirtz, PhD,§ Gregor Weirich, MD,|| Hans-Jürgen Wester, PhD,§
Jürgen E. Gschwend, MD,† Markus Schwaiger, MD,* Margret Schottelius, PhD,§ and Matthias Eiber, MD*

Purpose: The aim of this study was to evaluate the detection efficiency of ^{111}In-PSMA-I&T SPECT/CT in comparison to hybrid ^{68}Ga-PSMA HBED-CC PET in patients with early recurrent prostate cancer.

Methods: Twenty-two patients (mean age, 68.2 ± 6.8 years; range, 52–76 years) with rising prostate-specific antigen (PSA; median, 1.03 ng/mL; range, 0.2–7.2 ng/mL) and known positive lesions in hybrid ^{68}Ga-PSMA HBED-CC PET scheduled for salvage surgery were included. Whole-body scintigraphy and SPECT/CT were performed 4 hours after application of 147.0 ± 24.8 MBq (range, 90–183 MBq) ^{111}In-PSMA I&T. Images were evaluated for suspected lesions, and conspicuity of all lesions was rated using a 4-point-scale (0 = not seen, 1 = retrospectively seen in knowledge of ^{68}Ga-PSMA HBED-CC PET, 2 = low signal, 3 = high signal). Tumor-to-background ratios were determined for SPECT and PET and compared. Tumor-to-background ratio of SPECT was correlated with lesion size as well as patients' Gleason score and PSA level.

Results: ^{111}In-PSMA I&T SPECT/CT detected 14 of 29 PET-positive lesions (48.3%) with no additional lesions identified with ^{111}In-PSMA I&T SPECT/CT. There was a significant weak to moderate correlation of PSA level with tumor-to-background ratio of ^{111}In-PSMA I&T SPECT/CT (correlation coefficient r = 0.6406; 95% confidence interval, 0.1667–0.8741; P = 0.0136). There was no significant difference (P > 0.05), but a weak trend toward a higher detectability in ^{111}In-PSMA I&T SPECT/CT regarding lesion size and initial PSA level.

Conclusions: In a preselected collective of recurrent prostate cancer patients with low PSA values, ^{111}In-PSMA I&T SPECT/CT showed lower detection rates than hybrid ^{68}Ga-HBED-CC PSMA PET. However, ^{111}In-PSMA I&T SPECT/CT showed a patient based detection rate of 59%, making it a potentially valuable imaging tool where PET is not available apart from its proven value as a PSMA-targeted probe for radioguided surgery.

Key Words: ^{111}In-PSMA I&T, biochemical recurrence, hybrid imaging, prostate cancer, PSMA ligand, SPECT/CT

(*Clin Nucl Med* 2016;41: e397–e402)

Prostate cancer (PC) is the most frequent tumor entity in men, and the development of tumor recurrence after initial curative treatment is an important problem in clinical management.[1–3] Therefore, the early and sensitive detection of recurrent disease is essential for further therapeutic management. CT and MRI, as well as functional PET imaging using radiolabeled choline derivatives, often underestimate the extent of metastatic spread.[4,5] Because prostate-specific membrane antigen (PSMA) is known to be overexpressed in PC and its metastases, efforts have been made to develop ligands for this target.[6] Recently, ^{68}Ga-PSMA-HBED-CC, a PSMA inhibitor targeting the extracellular located active center of PSMA, has been introduced with promising results.[7,8] Several studies showed increased detection rates in patients with biochemical recurrence after radical prostatectomy (RPE) compared with tracers such as ^{18}F-choline, especially at low prostate-specific antigen (PSA) values.[9,10] In addition, high sensitivity and specificity were reported for ^{68}Ga-PSMA-HBED-CC PET in the setting of primary lymph node (LN) staging in patients with intermediate- to high-risk PC.[11] However, PET is not as widely available as scintigraphy and SPECT; thus, a PSMA-targeting compound for scintigraphy is of special interest. In addition to ^{68}Ga-PSMA-HBED-CC, another PSMA-binding inhibitor, PSMA I&T (I&T for "imaging and therapy"), has been successfully developed and evaluated as ^{68}Ga- and ^{177}Lu-labeled compounds in preclinical and first clinical studies.[12–15] Because this ligand is based on a DOTAGA chelator, we aimed to exploit this derivative for ^{111}In-labeling and first evaluation as SPECT agent. In patients with minimal or localized metastatic tumor, load salvage concepts are increasingly favored as they influence progression-free survival positively.[16,17] However, intraoperative identification of small metastatic LN detected by ^{68}Ga-PSMA HBED-CC PET is often difficult. Therefore, radioguided surgery (RGS) using ^{111}In-PSMA-I& has been introduced and was shown to be of high value for intraoperative detection of metastatic PC lesions.[18] Besides its suitability for RGS, ^{111}In-PSMA I&T may also be useful for preoperative planar scintigraphy and/or SPECT/CT imaging to visualize tumor

deposits. The aim of our study was therefore to evaluate the suitability of ^{111}In-PSMA I&T SPECT/CT for sensitive detection of early recurrent PC lesions. For comparison, hybrid ^{68}Ga-PSMA HBED-CC PET was performed in the same patients and was used to cross-validate SPECT/CT findings.

MATERIALS AND METHODS

Patients

In this retrospective analysis, 22 patients (mean age, 68.2 ± 6.8; range, 52–76 years) with rising PSA (median, 1.03 ng/mL; range, 0.2–7.2ng/mL) and ^{68}Ga-PSMA HBED-CC PET-positive LN scheduled for salvage lymphadenectomy using RGS were included. Inclusion criteria were previous biochemical recurrence after primary therapy such as RPE (n = 20), radiation therapy (n = 1), or high-intensity focused ultrasound (n = 1). None of the patients had received androgen deprivation therapy within the last 6 months prior to the examination. Patient characteristics are summarized in Table 1. The retrospective evaluation of the study was approved by the ethics committee of the Technical University Munich (permit 145/15). The serum PSA level at the time of the PET examination as well as histopathology was available in all patients. Gleason score was available in 20 of 22 patients.

Synthesis and Application of ^{111}In-Labeled PSMA I&T and ^{68}Ga-PSMA-HBED-CC

^{111}In-PSMA I&T

The synthesis of PSMA I&T (DOTAGA-(I-y)fk(Sub-KuE) was performed as described previously.[13] For ^{111}In-labeling, 500 μL of [^{111}In]InCl$_3$ (SA >205 GBq/μmol; Mallinckrodt

Pharmaceuticals, Dublin, Ireland) was added to 14 μL PSMA I&T (1.0 mM in water) in 600 μL sodium acetate buffer (0.15 M, pH 5.7). After heating to 95°C for 25 minutes, labeling was quantitative. The reaction mixture was purified over a Waters Sep Pak C18 light cartridge (Waters Corporation, Milford, MA). The final product was dissolved in 8.5 mL phosphate-buffered saline with subsequent sterile filtration.

^{68}Ga-PSMA HBED-CC

^{68}Ga-PSMA HBED-CC was labeled with [68]Ga^{3+} (half-life 67.6 minutes) from a [68]Ge/^{68}Ga radionuclide generator (iThemba Labs, Gauteng, South Africa) by means of a fully automated module (GRP; Scintomics, Fürstenfeldbruck, Germany) and a GMP-grade disposable cassette and reagent kit (ABX, Radeberg, Germany). The final product was diluted with phosphate-buffered saline and sterile filtered. Variation of injected radiotracer activity was caused by the short half-life of ^{68}Ga and variable elution efficiencies obtained during the lifetime of the [68]Ge/^{68}Ga radionuclide generator.

Imaging Protocol

^{111}In-PSMA I&T Scintigraphy and SPECT/CT

All patients received an intravenous injection of 147.0 ± 24.8 MBq (range, 90–183 MBq) ^{111}In-labeled PSMA I&T, and whole-body scintigraphy and SPECT/CT were acquired 4 hours post injectionem (p.i.) on a Siemens Symbia T6 instrument (Siemens Medical Solutions, Erlangen, Germany). Planar whole-body images were acquired with continuous table feed of 10 cm/min. SPECT/CT images were acquired immediately after the planar images. The SPECT/CT system consisted of a dual-head variable-angle γ-camera equipped with medium-energy high-resolution collimators and a multislice spiral CT component optimized for rapid rotation. The SPECT acquisition (64 × 64 matrix, 64 frames, 30 s/frame) was performed using 6 angular steps in a 20-second time frame. For CT (130 kV, 15 mAs), 5-mm slices were obtained.

^{68}Ga-PSMA HBED-CC PET Imaging

PET acquisition was started at a mean time of 57.2 ± 12.3 minutes (range, 45–89 minutes) after intravenous application of 165.9 ± 29.8 MBq ^{68}Ga-PSMA HBED-CC (range, 99–206 MBq). Fourteen patients underwent ^{68}Ga-PSMA HBED-CC PET/CT on a Biograph mCT scanner (Siemens Medical Solutions) and 8 patients ^{68}Ga-PSMA HBED-CC PET/MR on a Biograph mMR scanner (Siemens Medical Solutions). PET/CT and PET/MR acquisitions were performed as previously described.[19,20] For PET/CT, emission time was 4 minutes per bed position, whereas in PET/MR emission time for the trunk was 5 minutes per bed position. All PET images were acquired in 3-dimensional mode and reconstructed by an attenuation-weighted ordered-subsets expectation maximization algorithm (4 iterations, 8 subsets) followed by a postreconstruction smoothing Gaussian filter (5-mm full width at half maximum).

Mean time interval between ^{68}Ga-PSMA HBED-CC PET and ^{111}In-PSMA I&T SPECT/CT was 57 ± 34 days (median, 50 days). Twenty-four hours after injection of ^{111}In-PSMA I&T, all patients underwent RGS as an individual treatment concept after having obtained informed consent.

Image Analysis

For image analysis, all data sets were transferred to a dedicated postprocessing workstation (Syngo MMWP; Siemens Medical Solutions). All images from whole-body scintigraphy, SPECT/CT, PET/CT, or PET/MR were read by 1 nuclear medicine physician and 1 radiologist in consensus.

TABLE 1. Patient Characteristics

Patient No.	Age, y	Primary Therapy	Gleason Score	PSA, ng/mL	Findings PET	Findings SPECT/CT
1	58	RPE	—	0.45	1 LNM	1 LNM
2	69	RPE	7	0.40	1 LNM	1 LNM
3	69	RPE	7	2.58	1 LNM, 1 LR	—
4	52	RPE	9	0.97	1 LNM	—
5	75	RPE	8	4.36	4 LNM	1 LNM
6	76	RPE	5	1.9	2 LNM	1 LNM
7	59	RPE	7	0.80	1 LR	—
8	71	RPE	5	1.90	1 LNM	1 LNM
9	72	RPE	7	4.70	2 LNM	1 LNM
10	76	RPE	9	0.76	1 LNM	—
11	75	RPE	7	0.46	1 LNM	1 LNM
12	60	RTX	6	1.08	1 LNM	1 LNM
13	75	RPE	8	0.50	1 LNM	1 LNM
14	66	RPE	9	0.27	1 LNM	—
15	67	RPE	7	1.33	1 LNM	1 LNM
16	74	HIFU	—	2.45	2 LNM	1 LNM
17	71	RPE	7	0.90	1 LR	—
18	73	RPE	8	0.20	1 LNM	—
19	71	RPE	8	7.20	1 LNM	1 LNM
20	66	RPE	7	0.74	1 LNM	—
21	66	RPE	5	1.28	1 LNM	—
22	59	RPE	6	1.46	1 LNM	1 LNM

HIFU indicates high-intensity focused ultrasound; LR, local recurrence; RTX, radiation therapy.

First, all PET-positive lesions suggestive of recurrent PC (local recurrence or LN metastasis [LNM]), as well as its localization, were noted. Any focal uptake of ^{68}Ga-PSMA HBED-CC higher than the surrounding background and not associated with physiological uptake (eg, bladder, ureter) was considered suggestive of malignancy. An SUV analysis of tracer uptake in the suspected lesions was performed by using an isocontour VOI including all voxels greater than 50% of the maximum covering the whole lesion volume. For quantitative comparison, a tumor-to-background ratio (TBR) was determined for PET-positive lesions with the muscle adjacent to the suspected lesions serving as reference. The muscle was evaluated on 3 consecutive images based on a freehand surface ROI. In addition, in every morphological data set (CT or MRI), its size in millimeters was measured.

First, ^{111}In-PSMA I&T whole-body scintigraphy and SPECT/CT were evaluated with a time interval of at least 4 weeks. In a second step, ^{111}In-PSMA I&T SPECT and ^{68}Ga-PSMA HBED-CC PET were analyzed side-by-side to rate potential additional lesions prospectively only perceptible in PET. Lesion detectability in ^{111}In-PSMA I&T SPECT was rated as follows: 0 = not seen, 1 = retrospectively seen in knowledge of ^{68}Ga-PSMA HBED-CC PET, 2 = low signal, 3 = high signal. To calculate the average counts within the tumor on SPECT/CT images, a round 3-dimensional isocontour ROI including all voxels greater than 50% of the maximum was created covering the whole lesion volume. For quantitative comparison, TBR was determined for ^{111}In-PSMA I&T–positive lesions with the muscle adjacent to the tumor serving as reference as stated previously.

Statistical Analysis

All statistical analyses were performed using MedCalc software (version 13.2.0, 2014; MedCalc, Ostend, Belgium). Descriptive statistical evaluation was performed with all data expressed as mean value ± SD (range). Differences in lesion size as well as patients' Gleason score and initial PSA level of ^{111}In-PSMA I&T SPECT and ^{68}Ga-PSMA HBED-CC PET were compared by using 2-sample Student t test. In addition, TBR of ^{68}Ga-PSMA HBED-CC PET and ^{111}In-PSMA I&T SPECT/CT was correlated (correlation coefficient r, P value, and 95% confidence interval). Differences were deemed to be significant at $P < 0.05$.

RESULTS

In total, 29 lesions in 22 patients were identified with ^{68}Ga-PSMA HBED-CC PET. Twenty-six of those 29 lesions were classified as LNM and 3 lesions as local recurrence (Table 1). PET-positive lesions had a mean diameter of 8 ± 4 mm (range, 3–20 mm) with a mean SUV of 7.3 ± 5.3 (range, 2.0–20.6).

^{111}In-PSMA I&T SPECT/CT detected 14 (48.3%) of 29 PET-positive lesions in 13 (59%) of 22 patients. Eleven lesions presented with a high signal (rating 3) and 3 lesions with a low signal (rating 2). A total number of 15 PET-positive lesions were not detectable in ^{111}In-PSMA I&T SPECT/CT, neither prospectively nor retrospectively in knowledge of the PET results. Compared with ^{68}Ga-PSMA HBED-CC PET, no additional lesions were identified with ^{111}In-PSMA I&T SPECT/CT.

There was no correlation of TBR between ^{68}Ga-PSMA HBED-CC PET and ^{111}In-PSMA I&T SPECT/CT (correlation coefficient $r = 0.09887$; 95% confidence interval, −0.4556 to 0.5981; $P = 0.7367$; Fig. 1A). However, there was a statistically significant but only weak to moderate correlation between PSA level and TBR of ^{111}In-PSMA I&T SPECT/CT (correlation coefficient $r = 0.6406$; 95% confidence interval, 0.1667–0.8741; $P = 0.0136$; Fig. 1B). Lesion size (correlation coefficient $r = 0.01499$; 95% confidence interval, −0.5197–0.5413; $P = 0.9594$) and Gleason score (correlation coefficient $r = 0.3193$; 95% confidence interval, −0.3117–0.7549; $P = 0.3116$) did not show any correlation with TBR of ^{111}In-PSMA I&T SPECT/CT.

There was no significant difference ($P > 0.05$) but a slow trend toward a higher detectability in ^{111}In-PSMA I&T SPECT/CT with increasing lesion size. The mean diameter of PET-positive lesions clearly visible in ^{111}In-PSMA I&T SPECT/CT and presenting with a high signal (rating 3) was 9.64 ± 5.20 mm (range, 3–20 mm), whereas lesions with a low signal (rating 2) in ^{111}In-PSMA I&T SPECT/CT showed a mean lesion size of 8.5 ± 1.29 mm (range, 7–10 mm). Lesions not being detectable in ^{111}In-PSMA I&T SPECT/CT showed a mean diameter of 6.17 ± 2.55 mm (range, 3–12 mm).

For ^{111}In-PSMA I&T SPECT/CT, a slow trend toward a higher detectability in patients with higher PSA values was present; hence, no statistical correlation could be found. The PSA value of patients with PET-positive lesions and presenting with a high signal (rating 3) in ^{111}In-PSMA I&T SPECT/CT was 2.7 ± 2.2 ng/mL (range, 0.4–7.2 ng/mL), whereas patients with only a low signal (rating 2) in ^{111}In-PSMA I&T SPECT/CT demonstrated a PSA value of 1.9 ± 1.9 ng/mL (range, 0.5–4.4 ng/mL). Patients with lesions not detected in ^{111}In-PSMA I&T SPECT/CT presented with a PSA value of 1.51 ± 1.15 ng/mL (range, 0.2–4.4 ng/mL).

Representative ^{111}In-PSMA I&T SPECT/CT and ^{68}Ga-PSMA HBED-CC PET images of 2 patients with LNM in the pelvis are shown in Figures 2 and 3. While the LNM can be easily identified with both ^{111}In-PSMA I&T SPECT/CT and ^{68}Ga-PSMA HBED-CC PET in Figure 2, the LN in Figure 3 can only be identified as LNM with ^{68}Ga-PSMA HBED-CC PET. Note the difference in lesion size between both LNs.

Radioguided surgery with histopathologic evaluation of the specimens served as standard of reference showing LNM/local
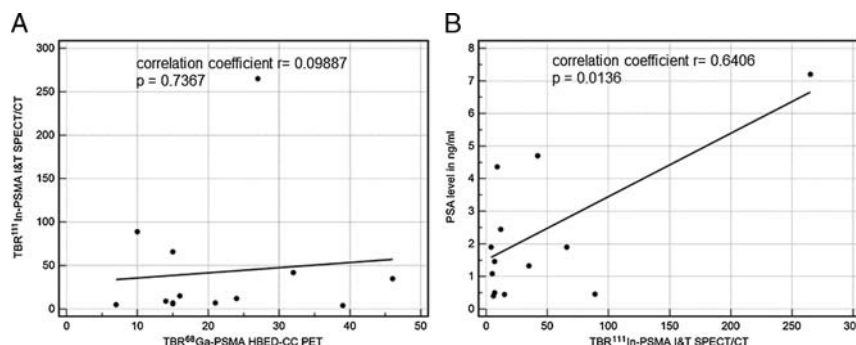
FIGURE 1. Correlation analysis of TBR of ^{111}In-PSMA I&T SPECT/CT and ^{68}Ga-PSMA HBED-CC PET (**A**) and TBR of ^{111}In-PSMA I&T SPECT/CT and PSA level (**B**).
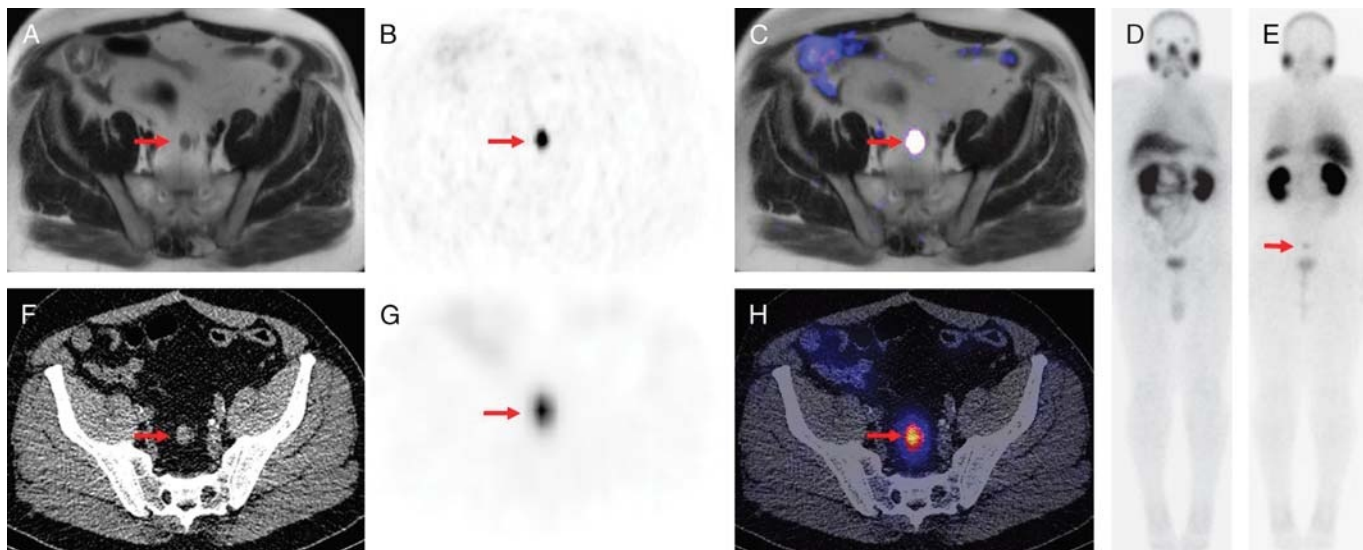
FIGURE 2. Example of ^{68}Ga-PSMA PET/MR (**A–C**) and ^{111}In-PSMA-I&T (**D–H**) of a 67-year-old patient (patient 15) with recurrent PC (PSA level, 1.33 ng/mL; Gleason score = 7). Axial T2-weighted MRI shows an enlarged presacral LN (red arrow in **A**; short axis, 14 mm). Simultaneously performed axial ^{68}Ga-PSMA ligand PET (red arrow in **B**) and axial ^{68}Ga-PSMA-HBED-CC PET/MRI fusion images (red arrow in **C**) show a distinct signal of this LN highly suggestive of metastasis that was proven by histology after ^{111}In-PSMA-I&T RGS. Preoperatively performed ^{111}In-PSMA-I&T shows concordant results with an intense focal uptake of the presacral LN in both whole-body planar scintigraphic images (red arrow in **D**; **E**) and SPECT/CT images (red arrow in **F–H**).

recurrence in all sites indicated by ^{68}Ga-PSMA HBED-CC PET. No false-positive findings were present.

DISCUSSION

In our study, detection rates using ^{111}In-PSMA I&T for SPECT/CT were considerably lower compared with ^{68}Ga-PSMA HBED-CC PET in patients with recurrent PC: Only 48.3% of the lesions being present in ^{68}Ga-PSMA HBED-CC PET could be detected with ^{111}In-PSMA I&T SPECT/CT. In 41% of the patients,

the lesions identified in ^{68}Ga-PSMA HBED-CC PET were not detectable using ^{111}In-PSMA I&T SPECT/CT. Despite a trend toward a higher detection rate in ^{111}In-PSMA I&T SPECT/CT regarding lesion size and PSA-level, no significant correlation could be observed.

Several factors may contribute to the observed lower sensitivity of ^{111}In-PSMA I&T SPECT/CT compared with ^{68}Ga-PSMA HBED-CC PET. One is certainly related to the principal technical differences between PET and SPECT imaging, leading to a highly superior spatial resolution of PET (4–6 mm) compared with SPECT
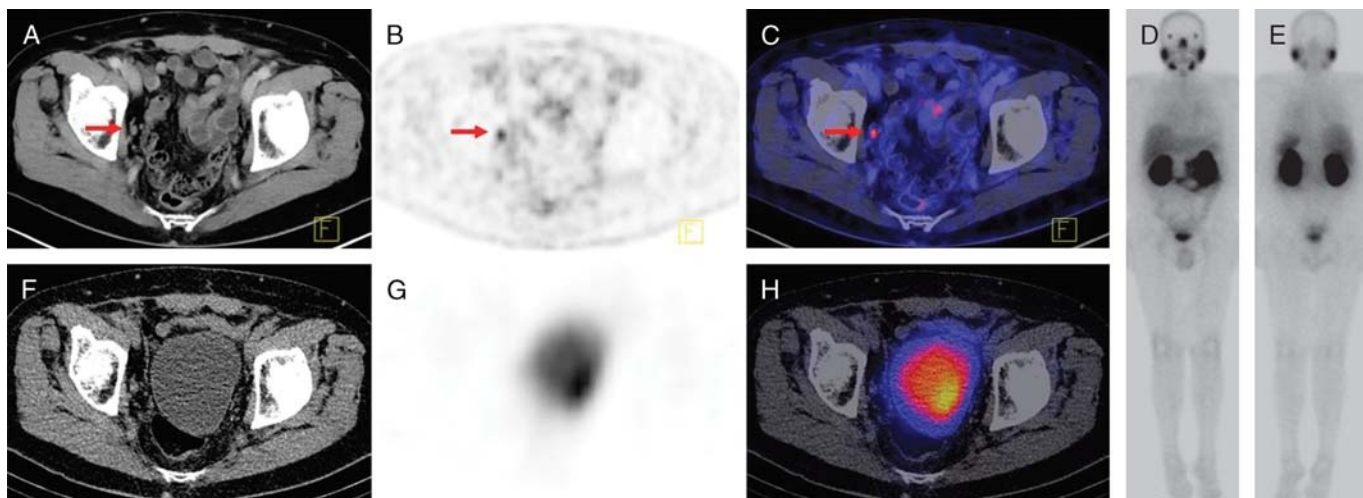
FIGURE 3. Axial ^{68}Ga-PSMA PET/CT images (**A–C**) and axial ^{111}In-PSMA-I&T (**D–H**) of a 76-year-old patient (patient 10) with recurrent PC (PSA level, 0.76 ng/mL; and Gleason score = 9). The LN in the right obturator fossa (red arrow in **A**) can be identified clearly as a metastasis despite its small size (short axis, 8 mm) because of the intense focal ^{68}Ga-PSMA uptake in PET of PET/CT (red arrow in **B**) and fused PET/CT (red arrow in **C**) (SUVmean/SUVmax, 3.5/5.1). However, preoperatively obtained ^{111}In-PSMA-I&T images show no uptake neither in the planar (**D, E**) or in the tomographic SPECT/CT images (**F–H**). Note that this LN was identified correctly with ^{111}In-PSMA-I&T RGS and proved to be an LNM histologically.

(8–12 mm).[21] There are no prior studies directly comparing PSMA inhibitors using SPECT and PET imaging. However, our results can be put in context with somatostatin receptor imaging studies comparing ^{68}Ga-DOTATATE PET and ^{111}In-DTPA-octreotide scintigraphy (octreoscan). Similar to our study, ^{68}Ga-DOTATATE PET revealed significantly more lesions compared with SPECT.[22,23] Furthermore, ^{68}Ga-DOTATATE PET/CT provided additional information in 83% of the patients compared with octreoscan changing the clinical management in a majority of patients.[22,24,25] However, for these agents, it is known that the targeting efficiency of octreoscan is clearly inferior to that of DOTATATE. Reubi et al[26] reported that the affinity of octreotide in binding somatostatin receptors is approximately 10-fold lower than that of DOTATATE. In comparison to our study, recent studies have shown that the PSMA affinity of ^{111}In-PSMA I&T and the ^{68}Ga compounds of PSMA are comparable. Therefore, the technical differences of PET and SPECT are most likely the main factors for lesion detection.[27]

Furthermore, the spatial resolution in ^{111}In-PSMA I&T SPECT/CT is further challenged by the comparably high gamma energy of [111]In (245 keV). Similar to reports from ^{111}In-octreotide, limiting factors of gamma imaging using ^{111}In-isotopes could be low image quality; high physiological uptake, which restricts detection of small lesions; prolonged imaging protocol; and relatively high radiation dose to the patients.[28] In addition, differences in tracer uptake and overall tracer kinetics between ^{68}Ga-PSMA HBED-CC and ^{111}In-PSMA I&T also might contribute to the observed differences in the achievable TBRs for the PET and SPECT radiopharmaceuticals, respectively. However, preclinical data on ^{111}In-PSMA I&T and ^{68}Ga-PSMA HBED-CC have demonstrated comparable PSMA affinity and nearly identical in vivo uptake and in vivo kinetics in LNCaP-tumor xenografts.[27] Furthermore, ^{68}Ga-PSMA I&T and ^{177}Lu-PSMA I&T have been found to be valuable radiopharmaceuticals with rapid clearance and low background activity in first patient studies.[12]

Potential alternative to ^{111}In-labeled PSMA inhibitors is the use of ^{99m}Tc-labeled agents. Recent studies report on novel ^{99m}Tc-labeled small-molecule PSMA inhibitors binding with high affinity to PSMA-positive tumor cells in vitro and in PC xenografts.[29] In a recently published study of Vallabhajosula et al[30] in patients with metastatic PC and in control subjects, those PSMA inhibitors were able to identify most bone metastases and soft-tissue PC lesions including subcentimeter LNs in comparison to bone scanning. However, those ^{99m}Tc-labeled small-molecule PSMA inhibitors have not been evaluated in depth and especially not in patients with early recurrent disease. Therefore, further studies correlating imaging findings with histopathology are pending.

Previously, studies have been published evaluating an ^{111}In-labeled, PSMA-directed antibody targeting the intracellular domain of PSMA (ProstaScint) in contrast to our PSMA ligand binding at the extracellular active center. Sensitivity, specificity, and overall accuracy of ProstaScint have been reported to be 75%, 86%, and 81%, respectively, with histopathology serving as criterion standard.[31] A study of Raj et al[32] showed that it may localize even early serum PSA recurrence after RPE. However, in that study, no histological confirmation and only limited and variable clinical follow-up data were available. A more recent study revealed that contrary to previous reports for patients with biochemical relapse after RPE presalvage ProstaScint scan findings outside the prostate fossa were not predictive of biochemical control after radiation therapy.[33] This might be related to the insufficient detection of small tumor deposits consequently not being taken into account for radiation therapy planning. However, although ProstaScint and ^{111}In-PSMA I&T are both ^{111}In labeled, pharmacokinetics and targeting strategy differ so fundamentally that no direct comparison is possible.

In our study, there was only a weak correlation between PSA level and TBR of ^{111}In-PSMA I&T SPECT/CT. This can be due to the high variance of lesion uptake, which is not related to the PSA level as indicated by a recent study of Afshar-Oromieh et al.[9] When grouping lesions in lesions with no, low, and high signal, lesions presenting with high signal had the tendency to be larger compared with those with low or no signal. However, the difference was not significant, probably based on the variable PSMA expression and/or the small sample size.

Interestingly, no correlation of TBR between ^{68}Ga-PSMA HBED-CC PET and ^{111}In-PSMA I&T SPECT/CT could be observed. This might again be due to the principal differences between SPECT and PET (different geometry, imaging with collimator in SPECT, count sensitivity, etc) and the different imaging characteristics of ^{68}Ga and [111]In. In addition, the imaging time point for the ^{68}Ga-PSMA HBED-CC PET scan (1 hour p.i.) has been clinically established as optimal considering tracer uptake and excretion kinetics.[34] In contrast, the optimal time window for imaging with ^{111}In-PSMA I&T has not yet been identified yet, because detailed studies evaluating tracer kinetics in patients are still ongoing.

Generally, it has to be taken into account that in our study the patient collective was preselected by PET with only patients with low-volume recurrent disease (small tumor deposits visible in PET) suitable for salvage RGS included. Furthermore, patients presented with relatively low PSA levels (median, 1.03 ng/mL; range, 0.2–7.2ng/mL). Therefore, it may be hypothesized that the detection rate of PSMA-positive lesions using ^{111}In-PSMA I&T SPECT/CT might be enhanced at higher PSA levels. This effect has already been demonstrated in PET studies using ^{11}C-choline, in which the detection rate was shown to positively correlate with increasing PSA levels.[19]

It is worth mentioning that there was a relatively long time interval (mean, 57 ± 34 days) between ^{68}Ga-PSMA HBED-CC PET imaging and preoperatively performed ^{111}In-PSMA I&T SPECT/CT. However, in recurrent PC with low PSA values, there is usually only a very slow progression, and thus, no substantial "biological" difference was assumed to have arisen between both examinations. For the same reason, that is, negligible tumor progression during the time interval between both imaging studies, a significant increase in tumor burden, which may lead to a slight overestimation of the performance of ^{111}In-PSMA I&T SPECT/CT compared with ^{68}Ga-PSMA HBED-CC PET, seems highly improbable.

On the other side, for ^{68}Ga-PSMA HBED-CC PET, furosemide is routinely administered to reduce potential artifacts from insufficient scatter correction around the kidneys and the urinary bladder. ^{111}In-PSMA I&T SPECT/CT was performed without prior injection of furosemide, resulting in a fuller bladder with high activity levels, inducing potential spillover to the surrounding tissue. This could explain, together with the lower ability of SPECT imaging to detect small tumor deposits due to the inferior resolution compared with PET, why the local recurrence was not detected using ^{111}In-PSMA I&T SPECT in all 3 cases (Table 1). Certainly it could also affect detection of LNM located near the bladder. A further limitation might be the fact that SPECT/CT imaging was performed routinely only 4 hours p.i. with no 24- or 48-hour imaging performed, which could have offered reduced background activity and higher TBR (as known from, eg, ^{111}In-DTPA-octreotide). In a minority of the patients in our study, SPECT/CT images were also available 24 h p.i., but showed no substantial differences with respect to TBR as compared with the images obtained at 4 hours p.i.

CONCLUSIONS

As previously shown, ^{111}In-PSMA I&T has undisputed value as a PSMA-targeted probe for the sensitive intraoperative detection

and RGS of PSMA-positive lesions of recurrent PC. In this study, ^{111}In-PSMA I&T was evaluated with respect to its suitability as a SPECT imaging agent in patients with early recurrent PC and possible salvage options. In a direct intrapatient comparison, ^{111}In-PSMA I&T SPECT/CT showed lower detection rates than ^{68}Ga-HBED-CC PSMA PET and allowed only partial visualization of small tumor deposits identified via ^{68}Ga-HBED-CC PSMA PET. This finding, however, was not unexpected, given the "suboptimal" radionuclide characteristics of ^{111}In for SPECT and the inherent differences in sensitivity and resolution between SPECT and PET. Despite these challenges, ^{111}In-PSMA I&T SPECT/CT showed a patient-based detection rate of 59%, making it, although not competitive with ^{68}Ga-HBED-CC PSMA PET, a potentially valuable imaging tool where PET is not available.

REFERENCES

1. Siegel R, Ma J, Zou Z, et al. Cancer statistics, 2014. *CA Cancer J Clin*. 2014; 64:9–29.

2. Freedland SJ, Presti JC Jr, Amling CL, et al. Time trends in biochemical recurrence after radical prostatectomy: results of the SEARCH database. *Urology*. 2003;61:736–741.

3. Han M, Partin AW, Zahurak M, et al. Biochemical (prostate specific antigen) recurrence probability following radical prostatectomy for clinically localized prostate cancer. *J Urol*. 2003;169:517–523.

4. Umbehr MH, Müntener M, Hany T, et al. The role of ^{11}C-choline and ^{18}F-fluorocholine positron emission tomography (PET) and PET/CT in prostate cancer: a systematic review and meta-analysis. *Eur Urol*. 2013;64: 106–117.

5. Evangelista L, Guttilla A, Zattoni F, et al. Utility of choline positron emission tomography/computed tomography for lymph node involvement identification in intermediate- to high-risk prostate cancer: a systematic literature review and meta-analysis. *Eur Urol*. 2013;63:1040–1048.

6. Eder M, Eisenhut M, Babich J, et al. PSMA as a target for radiolabelled small molecules. *Eur J Nucl Med Mol Imaging*. 2013;40:819–823.

7. Schäfer M, Bauder-Wüst U, Leotta K, et al. A dimerized urea-based inhibitor of the prostate-specific membrane antigen for ^{68}Ga-PET imaging of prostate cancer. *EJNMMI Res*. 2012;2:23.

8. Maurer T, Beer AJ, Wester HJ, et al. Positron emission tomography/magnetic resonance imaging with [68]Gallium-labeled ligand of prostate-specific membrane antigen: promising novel option in prostate cancer imaging? *Int J Urol*. 2014;21:1286–1288.

9. Afshar-Oromieh A, Zechmann CM, Malcher A, et al. Comparison of PET imaging with a (68)Ga-labelled PSMA ligand and (18)F-choline–based PET/CT for the diagnosis of recurrent prostate cancer. *Eur J Nucl Med Mol Imaging*. 2014;41:11–20.

10. Eiber M, Maurer T, Souvatzoglou M, et al. Evaluation of hybrid ^{68}Ga-PSMA ligand PET/CT in 248 patients with biochemical recurrence after radical prostatectomy. *J Nucl Med*. 2015;56:668–674.

11. Maurer T, Gschwend J, Wester HJ, et al. PET imaging with of prostate-specific membrane antigen (PSMA) for staging of primary prostate cancer with ^{68}Ga-HBED-PSMA. *J Clin Oncol*. 2015;68:530–504.

12. Weineisen M, Schottelius M, Simecek J, et al. [68]Ga- and 177Lu-labeled PSMA I&T: optimization of a PSMA-targeted theranostic concept and first proof-of-concept human studies. *J Nucl Med*. 2015;56:1169–1176.

13. Weineisen M, Simecek J, Schottelius M, et al. Synthesis and preclinical evaluation of DOTAGA-conjugated PSMA ligands for functional imaging and endoradiotherapy of prostate cancer. *EJNMMI Res*. 2014;4:63.

14. Herrmann K, Bluemel C, Weineisen M, et al. Biodistribution and radiation dosimetry for a probe targeting prostate-specific membrane antigen for imaging and therapy. *J Nucl Med*. 2015;56:855–861.

15. Baum RPKH, Volkmer B, et al. Theranostics of metastatic prostate cancer applying ^{177}Lu PSMA small molecules in combination with Ga-68 PSMA PET/CT. *Nuklearmediziner*. 2015:145–152.

16. Suardi N, Gandaglia G, Gallina A, et al. Long-term outcomes of salvage lymph node dissection for clinically recurrent prostate cancer: results of a single-institution series with a minimum follow-up of 5 years. *Eur Urol*. 2015;67:299–309.

17. Abdollah F, Briganti A, Montorsi F, et al. Contemporary role of salvage lymphadenectomy in patients with recurrence following radical prostatectomy. *Eur Urol*. 2015;67:839–849.

18. Maurer T, Weirich G, Schottelius M, et al. Prostate-specific membrane antigen-radioguided surgery for metastatic lymph nodes in prostate cancer. *Eur Urol*. 2015;68:530–534.

19. Krause BJ, Souvatzoglou M, Tuncel M, et al. The detection rate of [^{11}C] choline-PET/CT depends on the serum PSA-value in patients with biochemical recurrence of prostate cancer. *Eur J Nucl Med Mol Imaging*. 2008;35: 18–23.

20. Souvatzoglou M, Eiber M, Martinez-Moeller A, et al. PET/MR in prostate cancer: technical aspects and potential diagnostic value. *Eur J Nucl Med Mol Imaging*. 2013;40(suppl 1):S79–S88.

21. Khalil MM, Tremoleda JL, Bayomy TB, et al. Molecular SPECT imaging: an overview. *Int J Mol Imaging*. 2011;2011:796025.

22. Mojtahedi A, Thamake S, Tworowska I, et al. The value of (68)Ga-DOTATATE PET/CT in diagnosis and management of neuroendocrine tumors compared to current FDA approved imaging modalities: a review of literature. *Am J Nucl Med Mol Imaging*. 2014;15:426–434.

23. Krausz Y, Freedman N, Rubinstein R, et al. ^{68}Ga-DOTA-NOC PET/CT imaging of neuroendocrine tumors: comparison with ^{111}In-DTPA-octreotide (OctreoScan®). *Mol Imaging Biol*. 2011;13:583–593.

24. Srirajaskanthan R, Kayani I, Quigley AM, et al. The role of ^{68}Ga-DOTATATE PET in patients with neuroendocrine tumors and negative or equivocal findings on 111In-DTPA-octreotide scintigraphy. *J Nucl Med*. 2010;51:875–882.

25. Hofman MS, Kong G, Neels OC, et al. High management impact of Ga-68 DOTATATE (GaTate) PET/CT for imaging neuroendocrine and other somatostatin expressing tumours. *J Med Imaging Radiat Oncol*. 2012;56: 40–47.

26. Reubi JC, Schär JC, Waser B, et al. Affinity profiles for human somatostatin receptor subtypes SST1-SST5 of somatostatin radiotracers selected for scintigraphic and radiotherapeutic use. *Eur J Nucl Med*. 2000;27: 273–282.

27. Schottelius M, Wirtz M, Eiber M, et al. [(111)In]PSMA-I&T: expanding the spectrum of PSMA-I&T applications towards SPECT and radioguided surgery. *EJNMMI Res*. 2015;5:68.

28. Al-Nahhas A, Win Z, Szyszko T, et al. What can gallium-68 PET add to receptor and molecular imaging? *Eur J Nucl Med Mol Imaging*. 2007;34: 1897–1901.

29. Hillier SM, Maresca KP, Lu G, et al. ^{99m}Tc-labeled small-molecule inhibitors of prostate-specific membrane antigen for molecular imaging of prostate cancer. *J Nucl Med*. 2013;54:1369–1376.

30. Vallabhajosula S, Nikolopoulou A, Babich JW, et al. ^{99m}Tc-labeled small-molecule inhibitors of prostate-specific membrane antigen: pharmacokinetics and biodistribution studies in healthy subjects and patients with metastatic prostate cancer. *J Nucl Med*. 2014;55:1791–1798.

31. Hinkle GH, Burgers JK, Neal CE, et al. Multicenter radioimmunoscintigraphic evaluation of patients with prostate carcinoma using indium-111 capromab pendetide. *Cancer*. 1998;83:739–747.

32. Raj GV, Partin AW, Polascik TJ. Clinical utility of indium 111-capromab pendetide immunoscintigraphy in the detection of early, recurrent prostate carcinoma after radical prostatectomy. *Cancer*. 2002;94:987–996.

33. Thomas CT, Bradshaw PT, Pollock BH, et al. Indium-111-capromab pendetide radioimmunoscintigraphy and prognosis for durable biochemical response to salvage radiation therapy in men after failed prostatectomy. *J Clin Oncol*. 2003;21:1715–1721.

34. Afshar-Oromieh A, Malcher A, Eder M, et al. Reply to Reske et al.: PET imaging with a [^{68}Ga]gallium-labelled PSMA ligand for the diagnosis of prostate cancer: biodistribution in humans and first evaluation of tumour lesions. *Eur J Nucl Med Mol Imaging*. 2013;40:971–972.